Polymer Degradation and Stability 97 (2012) 1345–1354

Contents lists available at SciVerse ScienceDirect

Polymer Degradation and Stability

journal homepage: www.elsevier.com/locate/polydegstab

Biodegradability studies of poly(butylene succinate)/organo-montmorillonite nanocomposites under controlled compost soil conditions: Effects of clay loading and compatibiliser

Y.J. Phua [a,b], N.S. Lau [c], K. Sudesh [c], W.S. Chow [a,b], Z.A. Mohd Ishak [a,b,*]

[a] Cluster for Polymer Composites, Engineering and Technology Research Platform, Engineering Campus, Universiti Sains Malaysia, 14300 Nibong Tebal, Penang, Malaysia
[b] School of Materials and Mineral Resources Engineering, Engineering Campus, Universiti Sains Malaysia, 14300 Nibong Tebal, Penang, Malaysia
[c] Ecobiomaterial Research Laboratory, School of Biological Sciences, Universiti Sains Malaysia, 11800 Penang, Malaysia

ARTICLE INFO

Article history:
Received 16 March 2012
Received in revised form
17 April 2012
Accepted 21 May 2012
Available online 27 May 2012

Keywords:
Poly(butylene succinate)
Organo-montmorillonite
Nanocomposite
Biodegradability
Soil burial

ABSTRACT

Biodegradable nanocomposites were prepared from poly(butylene succinate) (PBS) and organo-montmorillonite (OMMT), in the presence of maleic anhydride-grafted PBS (PBS-g-MA) as compatibiliser. The effects of OMMT loading and PBS-g-MA on the biodegradability of PBS nanocomposites were investigated. Soil burial testing was carried out for 180 days in natural organic humus compost soil under controlled conditions. It is noted that the weight loss of nanocomposites was lower than that of neat PBS, due to the enhanced barrier properties after addition of OMMT. However, the addition of PBS-g-MA increased the weight loss of nanocomposite. The mechanical properties of PBS nanocomposites were significantly reduced after the soil burial. Biodegradation of the material was further confirmed by the decreased molecular weight through gel permeation chromatography (GPC), and changes in the chemical structure as verified by Fourier transform infrared (FTIR) spectroscopy. This was supported by the degraded surface of PBS and the nanocomposites observed under scanning electron microscopy (SEM). The effects of biodegradation on the thermal properties were studied through the differential scanning calorimetry (DSC). In addition, the biodegradation rate of the materials was determined by measuring the carbon dioxide (CO_2) evolution. The degraded samples were recovered and PBS-degrading bacteria were found to be present in the exposed samples.

1. Introduction

Over the last few decades, the usage of plastic materials has been growing progressively. Most of the conventional plastics are non-degradable and no naturally occurring microorganisms can break them down. The massive increase in the usage of plastic products as a consequence leads to significant environmental impact. Therefore, the substitution of these conventional non-degradable plastics with biodegradable plastics is of great interest to the society.

Aliphatic polyesters have been widely recognized as environmentally friendly biodegradable polymers. Poly(butylene succinate) (PBS) is one of the most promising biodegradable aliphatic polyesters, which was invented in the early 1990s by Showa Highpolymer in Japan. It is a competitive material against other biodegradable plastics due to its superior mechanical and thermal properties, good processability, high chemical resistance, availability and lower material cost [1–3]. Fujimaki [4] reported that the yield strength of PBS (Bionolle #1020) was 264% higher than that of low-density polyethylene (LDPE), and was 10.3% higher than that of polypropylene (PP). However, certain properties of PBS, such as softness, gas-barrier properties, melt viscosity for further processing, etc, are insufficient for numerous applications [1–3,5]. In our previous work, an organoclay, namely organo-montmorillonite (OMMT) was incorporated into PBS to produce nanocomposites and their enhanced mechanical, rheological and thermal properties were reported [6,7]. Furthermore, maleic-anhydride grafted PBS (PBS-g-MA) was added as compatibiliser in the PBS/OMMT nanocomposite system, in an attempt to further improve the properties of nanocomposites.

PBS, as biodegradable polyester, can be degraded under the natural environment by bacteria and fungi [8–11]. The field test of burying plastic or compositae samples in soil has been widely conducted for evaluating the biodegradation behaviour of biodegradable plastics [12–14]. Kim et al. [11] demonstrated the natural

* Corresponding author. Cluster for Polymer Composites, Engineering and Technology Research Platform, Engineering Campus, Universiti Sains Malaysia, 14300 Nibong Tebal, Penang, Malaysia. Tel.: +60 4 5995999; fax: +60 4 5941011.
E-mail addresses: zarifin@eng.usm.my, zarifin.ishak@gmail.com (Z.A. Mohd Ishak).

0141-3910/$ – see front matter © 2012 Elsevier Ltd. All rights reserved.
doi:10.1016/j.polymdegradstab.2012.05.024

soil burial test on PBS/agro-flour biocomposites and discovered that the properties of the biocomposites reduced drastically throughout the 120 days of soil burial. Liu et al. [15] found that significant weight loss occurred in the PBS composite reinforced with 10 wt% jute fibres after 180 days of compost-soil burial. However, detailed studies on the biodegradability of PBS/OMMT nanocomposites have not been reported. In the previous paper, degradation of PBS/OMMT nanocomposites under hydrolysis and hygrothermal ageing was reported [16]. As an extension of the previous work, this paper reports comprehensive studies on the biodegradation of PBS/OMMT nanocomposites under controlled compost soil conditions. The main focus of this study is on the effects of OMMT loading and addition of PBS-g-MA as compatibiliser on the biodegradability of nanocomposites. In addition, this research provides an intensive evaluation on the weight loss, mineralisation, chemical degradation, mechanical, thermal, as well as morphological properties of PBS and the nanocomposites after the soil burial test. Identification of microorganisms in the buried samples was also carried out.

2. Materials and methods

2.1. Materials

PBS (Bionolle #1020) was obtained from Showa Highpolymer Co., Ltd., Japan with MFI value of 25 g/10min (190 °C, 2.16 kg) and melting temperature of 115 °C. OMMT (Nanomer® I.30TC, Nanocor Inc, USA) with cation exchange capacity (CEC) of 110 mequiv/100 g, which contains MMT (70 wt%) intercalated by octadecylamine (30 wt%) was used in this study. Dicumyl peroxide (DCP) (Aldrich Luperox®) from Sigma–Aldrich Inc, USA was used as initiator. Maleic anhydride (MA) was supplied by R&M II Chemicals, USA.

2.2. Synthesis of PBS-g-MA

PBS-g-MA was used as compatibiliser in this study. First, PBS, MA and DCP were physically premixed in the composition of 100 phr, 10 phr and 1.5 phr, respectively. The reactive grafting process was performed in an internal mixer (Haake Polydrive R600, Germany) at 135 °C for 7 min, at a rotation speed of 50 rpm. The resulting PBS-g-MA was then subjected to purification by refluxing in chloroform for 4 h, and the hot solution was filtered into cold methanol. The precipitated polymer was then washed with methanol for several times, in order to remove any unreacted reagents, followed by drying in an oven at 60 °C for 24 h.

2.3. Preparation of nanocomposites

The PBS/OMMT nanocomposites were prepared via melt-mixing process in an internal mixer (Haake PolyDrive R600, Germany) at 135 °C for 5 min at a rotation speed of 50 rpm. The sample designations are presented in Table 1. The nanocomposite was then moulded in a compression moulding machine (GT 7014-A30C, Taiwan) at 135 °C and 3 min into dumbbell specimens.

Table 1
Sample designations of PBS and the nanocomposites.

Component (wt%)	PBS	PBS/ 2%OMMT	PBS/ 10%OMMT	PBS/ 2%OMMT/MA
PBS	100	98	90	93
OMMT	–	2	10	2
PBS-g-MA	–	–	–	5

2.4. Soil burial test

Soil burial test was conducted by burying the dumbbell specimens in a natural organic humus compost soil supplied by Engco Compost Enterprise, Malaysia. It is a soil enriched with mature compost, which consists of crushed tree bark, organic matter, sand and moisture. The compost soil contained 0.89% nitrogen, 4.76% phosphorus, 0.32% potassium, and with a pH of 7.46. The specimen was buried in the compost soil and incubated in a closed chamber, away from ultraviolet (UV) light, at an environmental temperature of 30 ± 2 °C and 60–70% relative humidity. Water was supplied constantly to keep the compost soil humid. A total of 30 specimens were buried for each compound, and five specimens from each compound were removed from the soil without replacement at 10, 30, 60, 90, 120 and 180 days for post-exposure characterizations.

2.5. Weight loss analysis

Each specimen was dug out periodically, washed with distilled water and dried to a constant weight at 60 °C in a vacuum oven. The percentage of weight loss was measured using an electronic balance and calculated by using Equation (1).

$$\text{Weight loss}(W_{\text{loss}}) = \frac{W_{\text{initial}} - W_{\text{final}}}{W_{\text{initial}}} \times 100\% \quad (1)$$

where, W_{initial} and W_{final} is the weight of sample before and after soil burial test. Five measurements were conducted for each compound.

2.6. Mechanical properties

After soil burial, mechanical tests were performed on the samples using universal testing machine (Instron 3366, Instron Co., Ltd., USA) at 23 ± 2 °C and 50 ± 5% relative humidity. Tensile test was carried out according to ASTM D638-03 (Type IV) with a gauge length of 50 mm and a cross-head speed of 5 mm/min. Five measurements were conducted for each compound.

2.7. Scanning electron microscopy (SEM)

The surface morphology of the samples was observed under a field-emission scanning electron microscope (FESEM) (Zeiss LEO Supra 35VP, Germany) operated at 10 kV. Prior to the observations, the samples were sputter-coated with a thin layer of gold to avoid electrical charging during examination.

2.8. Differential scanning calorimetry (DSC)

The DSC analysis was carried out using Perkin–Elmer DSC-6 (USA) machine in a nitrogen atmosphere. Sample was heated from 30 °C to 150 °C at a heating rate of 10 °C/min. The sample was then cooled from 150 °C to 30 °C at the same heating rate. Next, second heating was performed from 30 °C to 150 °C. Finally, it was cooled to 30 °C. Degree of crystallinity (χ_c) was calculated by using the following equations: For pure PBS,

$$\chi_c = \frac{\Delta H_c}{\Delta H_m^0} \times 100\% \quad (2)$$

where ΔH_c = crystallization enthalpy of sample, ΔH_m^0 = melting enthalpy of 100% crystalline PBS (110.3 J/g).

For polymer nanocomposites,

$$\chi_c = \frac{\Delta H_c}{\Delta H_m^0 \left(1 - W_f\right)} \times 100\% \quad (3)$$

where W_f = weight fraction of fillers in the nanocomposite.

2.9. Fourier transform infrared (FTIR) spectroscopy

FTIR analysis was carried out at ambient temperature by using Perkin–Elmer Spectrum One FTIR Spectrometer (USA). It was performed through the scanning wavelength from 4000 to 550 cm^{-1} with 32 scanning times. Carbonyl, vinyl and hydroxyl index were calculated using the equations shown below:

$$\text{Carbonyl Index(CI)} = \frac{I_{1710-1713}}{I_{2945}} \quad (4)$$

$$\text{Hydroxyl Index(HI)} = \frac{I_{3423-3429}}{I_{2945}} \quad (5)$$

$$\text{Vinyl Index(VI)} = \frac{I_{917}}{I_{2945}} \quad (6)$$

where I represents the peak intensity. In this study, the peak at 2945 cm^{-1} was chosen as the reference peak.

2.10. Gel permeation chromatography (GPC)

The molecular weight of PBS was measured by GPC analysis. GPC analysis was performed at 40 °C on an Agilent Technologies 1200 Series GPC system (USA) equipped with a refractive index detector (RID) and SHODEX K-806M and SHODEX K-802 columns. The calibration of the columns was carried out using a polystyrene standard of known molecular weight and polydispersity. The samples were then dissolved in chloroform at ambient temperature, followed by filtration to eliminate the contaminants. Chloroform was used as the eluent with a flow rate of 0.8 ml/min, and the injected sample volume was 50 μl with a polymer concentration of 1 mg/ml. The weight-average molecular weight (M_w) and number-average molecular weight (M_n) were obtained from the GPC analysis. The polydispersity index (PDI) was calculated as M_w/M_n. The average number of random chain scissions per unit mass (n_t) was calculated by:

$$n_t = \frac{1}{M_n} - \frac{1}{M_{no}} \quad (7)$$

where M_{no} and M_n are the number-average molecular weight at zero and time t during ageing, respectively.

2.11. Carbon dioxide (CO_2) evolution

Carbon dioxide (CO_2) evolution during the soil burial test was measured in accordance with ASTM D5988. First, 500 mg of test specimen was placed in 300 g of soil and mixed thoroughly in a desiccator. 20 ml of 0.5N KOH in a 50 ml beaker, and 50 ml of distilled water in a 100 ml beaker were placed in the desiccator. Next, the desiccator was sealed and placed in a dark cabinet at 25 ± 2 °C. KOH solution was used to trap the CO_2 evolved while the distilled water was to maintain the humidity. KOH was titrated with 0.05 N hydrochloric acid (HCl) using phenolphthalein as indicator. Net CO_2 produced from the aerobic biodegradation of PBS and the nanocomposites was calculated by subtracting the CO_2 evolved in a blank soil from the CO_2 evolved in the mixture of soil and samples as shown below:

$$0.05 \times (B - V) \times 44 \quad (8)$$

where B corresponds to the volume (ml) of acid needed to titrate the KOH in the blank test, and V corresponds to the volume (ml) of acid needed to titrate the KOH in the soil burial test. The percentage of CO_2 evolution was calculated as shown below:

$$\frac{\text{mass of } CO_2 \text{ produced(mg)}}{\text{mass of } CO_2 \text{ theoretically produced(mg)}} \times 100\% \quad (9)$$

The CO_2 evolution was measured every 3 days for the first 30 days, and every 1–3 weeks for the following 150 days. Periodically, the desiccator was opened to replenish the air and replace the KOH solution.

2.12. Isolation and identification of bacterial strain

After soil burial, the samples colonized by microorganisms were transferred aseptically into universal bottles with forceps. The samples were washed and re-suspended gently with 5 mL of sterile saline. To isolate the microorganisms present in the samples, appropriate dilutions were made and the dilutions were plated on nutrient agar plates. The plates were incubated at 30 °C for up to 7 days to allow the growth of bacterial colonies. Colony polymerase chain reaction (PCR) was performed with primers BSF8 (5′–AGAGTTTGATCCTGGCTCAG–3′) and BSR1541 (5′–AAGGAGGTGATCCAGCCGCA–3′) [17], generating a PCR product corresponding to *Escherichia coli* 16S rDNA sequence at positions 8 and 1541. All reactions were carried out in 25 μL volumes, containing 5 μL of 5X PCR buffer, 2 mM $MgCl_2$, 0.2 mM of deoxynucleoside triphosphate, 1 μL of each forward and reverse primers and 1.25 U of Taq DNA polymerase (Promega, USA). The PCR was performed with an initial denaturation at 94 °C for 10 min, then denaturation at 94 °C for 30 s, annealing at 60 °C for 1 min and elongation at 72 °C for 2 min. The amplified PCR products were purified with Wizard® SV gel and PCR clean up system (Promega, USA) and the purified PCR products were sent to 1st BASE Laboratory (Malaysia) for sequencing. The obtained sequences were compared with the GenBank database by using Basic Local Alignment Search Tool (BLAST, National Center for Biotechnology Information).

3. Results and discussion

3.1. Weight loss analysis

Fig. 1 presents the percentage weight loss of PBS nanocomposites during 180 days of soil burial. At the initial stage, the

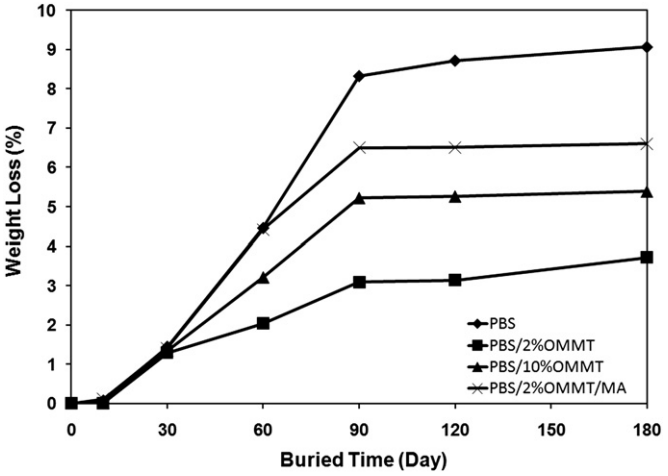

Fig. 1. Weight loss of PBS and the nanocomposites as a function of buried time.

weight loss increased rapidly as a function of exposure time. The rapid biodegradation rate at the initial stage is due to the degradation of low molecular weight fragments and exposed end groups in PBS [18]. The weight loss attained a steady state at 60 days and 90 days for nanocomposites and neat PBS, respectively. From Fig. 1, it can be seen that the weight loss of the PBS nanocomposites is lower as compared to the neat PBS. Similar observation was reported by Lee et al. [19] on the biodegradation of aliphatic polyester-based nanocomposites in compost. They claimed that the biodegradation was slow due to improvement of the barrier properties after nanocomposite preparation with clay, which restricted the penetration of microorganism through the material. Generally, barrier properties of polymer nanocomposites are highly dependent on the dispersion and distribution of OMMT platelets in the polymer matrix [20]. Based on our previous publication, a good intercalation and exfoliation of OMMT platelets in PBS/2%OMMT nanocomposites were observed, while agglomerations were found at higher OMMT loading, e.g. PBS/10%OMMT [6]. This indicates that the poor filler dispersion in PBS/10%OMMT nanocomposites may reduce the barrier properties, consequently leading to a higher biodegradability.

On the other hand, the addition of PBS-g-MA slightly increased the weight loss of the material, indicating a higher biodegradability in the compatibilised nanocomposites. It is possible that the low molecular weight of PBS-g-MA is responsible in enhancing the biodegradability. During soil burial, the moisture in the compost soil penetrated into the nanocomposites, subsequently reacting with the MA groups in PBS-g-MA to form an acid group through hydrolysis process. This acid group accelerated the chain scission of PBS, resulting in a higher biodegradability [21].

3.2. Mechanical properties

Loss in mechanical properties is one of the most relevant practical criterion to determine the degradation of a biodegradable material. Figs. 2–4 show the changes in mechanical properties as a function of soil burial time. Before soil burial, it was observed that tensile strength improved after the addition of 2 wt% OMMT, contributed by the good filler dispersion and distribution. The addition of PBS-g-MA as a compatibiliser into this nanocomposite further improved the tensile strength. The agglomerations at 10 wt % OMMT loading resulted in poor tensile strength of the nanocomposites, as discussed earlier [6]. From Figs. 2 and 3, a drastic decrease in the tensile strength and elongation at break is observed

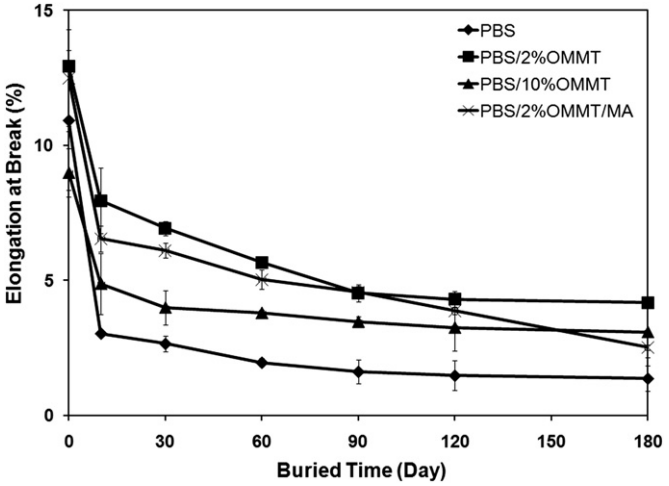

Fig. 3. Elongation at break of PBS and the nanocomposites as a function of buried time.

at 10–30 days of soil burial, followed by a gradual reduction throughout the 180 days of soil burial, respectively. The action of moisture and microorganism in soil caused the partial disruption of filler-matrix bonding, microcavities formation and followed by a random chain scission in the polymer chains. These eventually lead to a reduction in the tensile properties [16,22]. Highest tensile strength loss of 73.6% was observed in the neat PBS, followed by 56.3%, 51.8% and 43.8% for PBS/2%OMMT/MA, PBS/10%OMMT and PBS/2%OMMT. The elongation at break showed a similar trend. These results are in agreement with that of weight loss analysis.

Fig. 4 presents the effects of soil burial on the tensile modulus of PBS and the nanocomposites. It can be seen that the tensile modulus initially increased until 60 days of soil burial, due to the embrittlement effect after the material degrades. However, the tensile modulus decreased continuously after 60 days, indicating the severe degradation of mechanical properties after soil burial.

3.3. Scanning electron microscopy (SEM)

Fig. 5 reveals the surface morphology of PBS and the nanocomposites before and after the soil burial test. All the samples exhibit a relatively smooth and clear surface before soil burial. After

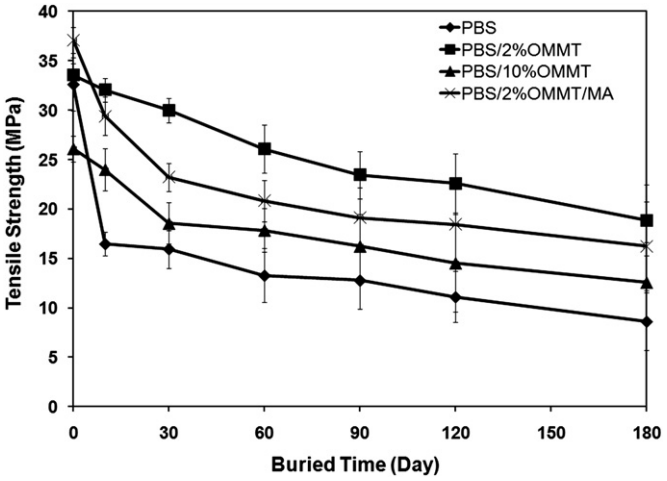

Fig. 2. Tensile strength of PBS and the nanocomposites as a function of buried time.

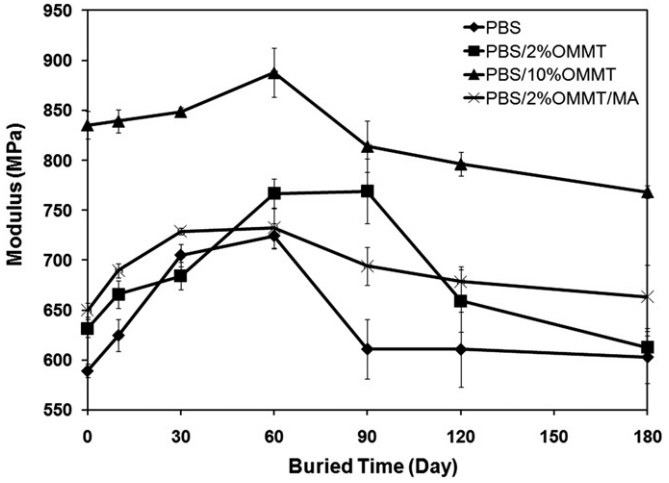

Fig. 4. Tensile modulus of PBS and the nanocomposites as a function of buried time.

180 days of soil burial, visible erosion was detected on the surface due to the biodegradation of PBS matrix, which caused permanent damage to the material. It is clear that the neat PBS and the compatibilised nanocomposites exhibited more significant surface erosion, corresponding to their higher biodegradation rate. Furthermore, the growth of microorganism was also detected on the sample surface as shown in Fig. 5b. Thus, observations from SEM micrographs provide clear evidence for the biodegradation of PBS and the nanocomposites.

3.4. Differential scanning calorimetry (DSC)

The effect of biodegradation on the thermal properties was investigated through DSC analysis, and the results are reported in Fig. 6 and Table 2. The DSC heating scan (Fig. 6a) clearly shows two distinct peaks, corresponding to the presence of two different types of crystalline lamella in PBS. The lower melting endotherm '*x*' is attributed to the melting of the original crystallites formed at the isothermal crystallisation temperature; while the higher melting

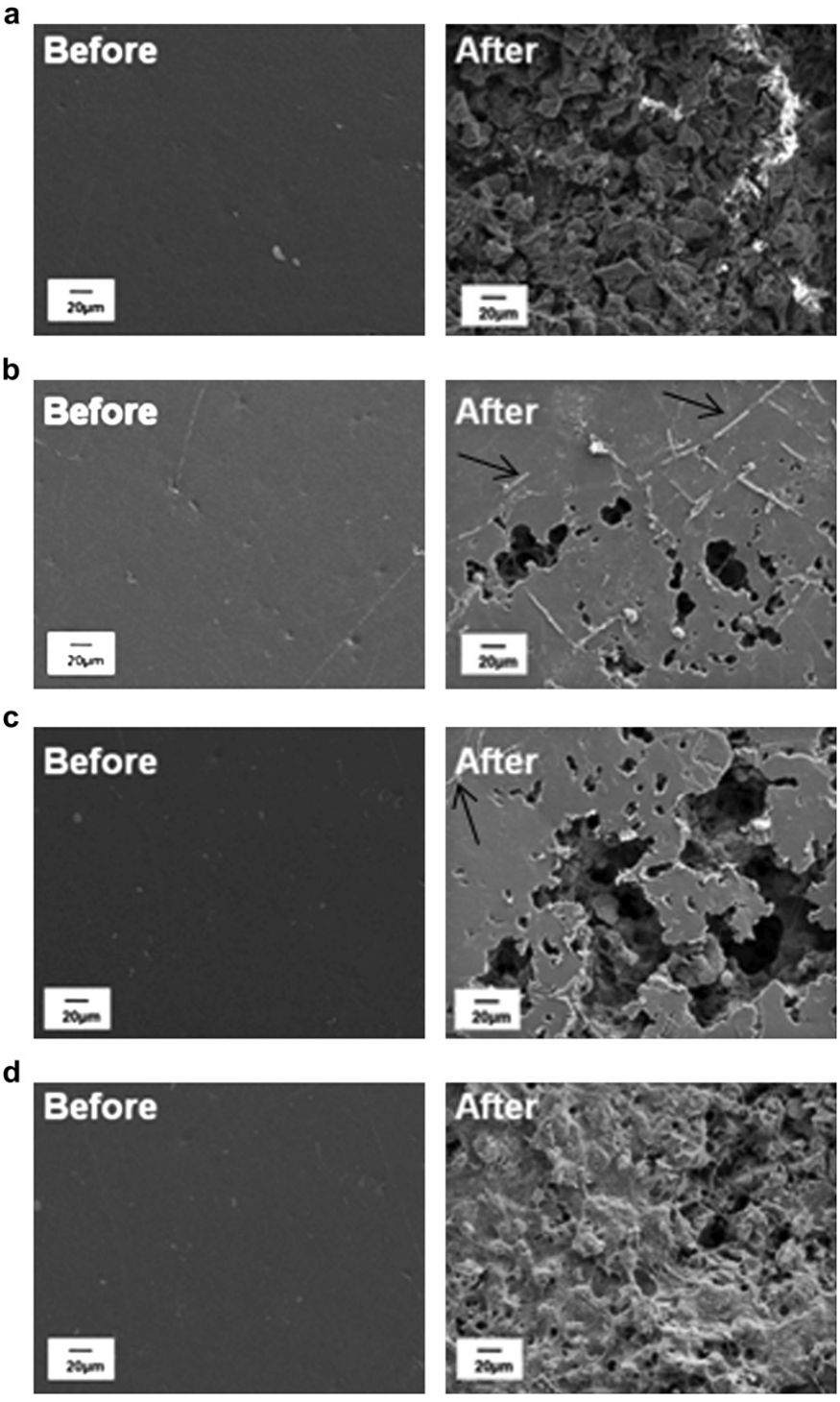

Fig. 5. SEM micrographs of (a) neat PBS, (b) PBS/2%OMMT, (c) PBS/10%OMMT and (d) compatibilised nanocomposites before and after 180 days soil burial.

endotherm '*y*' is due to the melting of the recrystallised crystals during the DSC analysis [23,24]. In addition, an exothermic peak that resulted from the fusion and recrystallisation of PBS crystals during heating was detected prior to *y*-endotherm [25]. There were no significant changes in the melting temperature (T_m) of PBS after incorporation of OMMT, while the $T_{m,x}$ was slightly enhanced with the addition of compatibiliser. This indicates that an interfacial chemical reaction has occurred between the anhydride group in PBS-g-MA and carbonyl group in PBS, which slightly enhanced the T_m of PBS crystals.

After 180 days exposure to soil burial, an obvious peak broadening was observed in the melting endotherm as shown in Fig. 6a. This is associated with the decreased degree of crystallinity (χ_c) in the material as reported in Table 2, which consequently leads to a lower melting enthalpy [26]. The T_m is slightly increased after the soil burial but the increment is rather low. Thus, it is believed that this phenomenon was not attributed to the exposure to soil, but related to the recrystallisation during the DSC scans that may affect to the crystal morphologies. This means that the effect of soil burial on T_m was insignificant.

Table 2 shows that the crystallization temperature (T_c) and χ_c decreased after 180 days of soil burial. The loss in the χ_c is of the same trend with the weight loss and the loss of mechanical properties, where the neat PBS suffers from the higher loss of χ_c. PBS is a semi-crystalline polymer. Basically, the biodegradation is expected to occur in the amorphous region at the initial stage, and finally in the crystalline regions [27]. The results revealed that degradation occurred in both the amorphous and the crystalline regions in PBS after 180 days soil burial, causing damage to the crystalline structure. Besides that, chemical impurities in the soil may penetrate into the molecular structure of polymers, subsequently suppressing the crystallization process [28]. The presence of these chemical impurities may also be responsible to the slight enhancement in T_m. The presence of PBS-g-MA increased the χ_c, owing to the action of PBS-g-MA as a heterogeneous nucleating agent. However, the enhanced biodegradability resulted in a drastic drop of the χ_c after 180 days of soil burial.

Table 2
DSC results for PBS and the nanocomposites before and after 180 days soil burial.

Compound	$T_{m,x}$ (°C)	$T_{m,y}$ (°C)	T_c (°C)	χ_c (%)
PBS (before)	102.2	112.4	85.8	57.6
PBS (after)	109.4	116.3	75.4	25.7
PBS/2%OMMT (before)	102.1	113.4	85.6	55.7
PBS/2%OMMT (after)	107.6	114.1	76.4	54.3
PBS/10%OMMT (before)	102.2	113.3	85.5	55.9
PBS/10%OMMT (after)	111.0	116.6	75.7	34.4
PBS/2%OMMT/MA (before)	107.4	113.6	82.1	65.9
PBS/2%OMMT/MA (after)	109.0	116.8	75.5	33.1

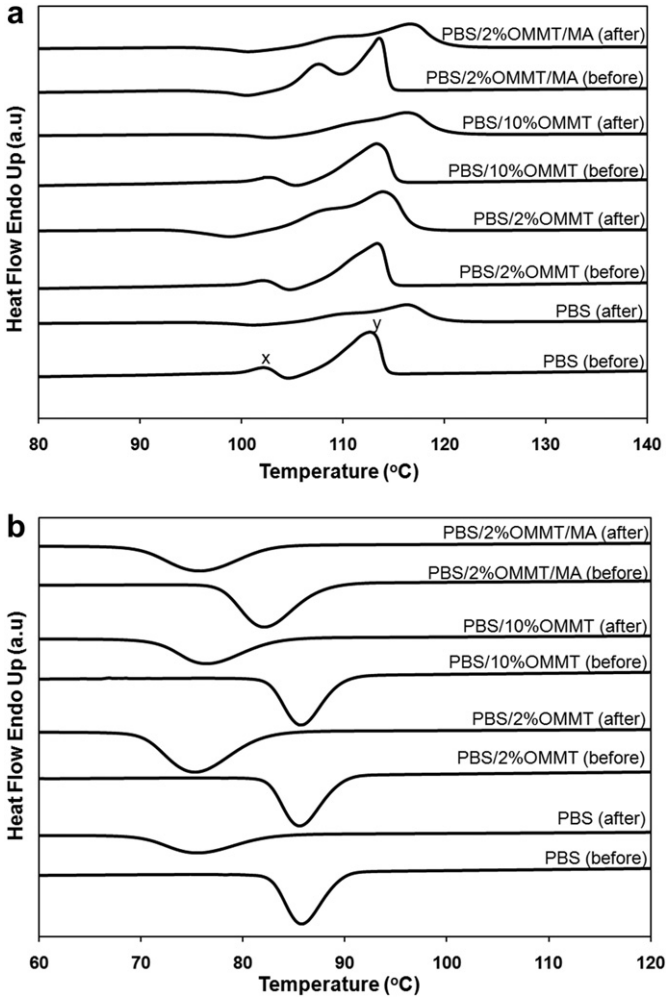

Fig. 6. DSC (a) melting and (b) cooling scans of PBS and the nanocomposites before and after 180 days soil burial.

3.5. Fourier transform infrared (FTIR) spectroscopy

Changes in chemical structure upon biodegradation were evaluated through FTIR spectroscopy. Fig. 7 displays the FTIR spectra of PBS and the nanocomposite at various soil burial times. Peaks in the range of 1144–1152 cm^{-1} corresponded to the –C–O–C– stretching in the ester linkages of PBS. The peaks at 1330 cm^{-1} and 2945 cm^{-1} were assigned to the symmetric and asymmetric deformational vibrations of $-CH_2-$ groups in the PBS main chains, respectively. Similar transmittance bands were observed in the PBS nanocomposites. The vibrations of the OMMT were recognized at the overlapping bands of 1042 cm^{-1} (Si–O), 880 cm^{-1} (Al–O–H), and 800 cm^{-1} (Al–Mg–O–H). In addition, the presence of octadecylamine as an intercalant in OMMT created additional peaks at 721–724 cm^{-1} (–NHR), which correspond to the stretching and deformation vibrations of the amine groups in octadecylamine [16,29].

From Fig. 7, it is worth noting that the samples exhibited increasing intensities after soil burial, typically at the bands of hydroxyl (3423–3429 cm^{-1}), carbonyl (1710–1713 cm^{-1}) and vinyl (917 cm^{-1}) groups. The broad band, which appears in the range of 3423–3429 cm^{-1} was due to the –OH stretching of hydroxyl groups in PBS and the OMMT surface. The band at the 1710–1713 cm^{-1} region was attributed to the C=O stretching vibrations of ester groups in PBS [16]. The presence of vinyl groups (CH_2=CH–) was also detected in the unsaturated region between 800 and 1000 cm^{-1}, which centred at the 971 cm^{-1} [30]. These bands are essential as the reference peaks in the identification of degradation products. Carbonyl index (CI), vinyl index (VI) and hydroxyl index (HI) were calculated and summarized in Table 3.

Table 3 shows that CI, VI and HI increased with the buried time at the initial stage until 60–90 days of soil burial. The increase in carbonyl groups formation after soil burial is known to be an effect

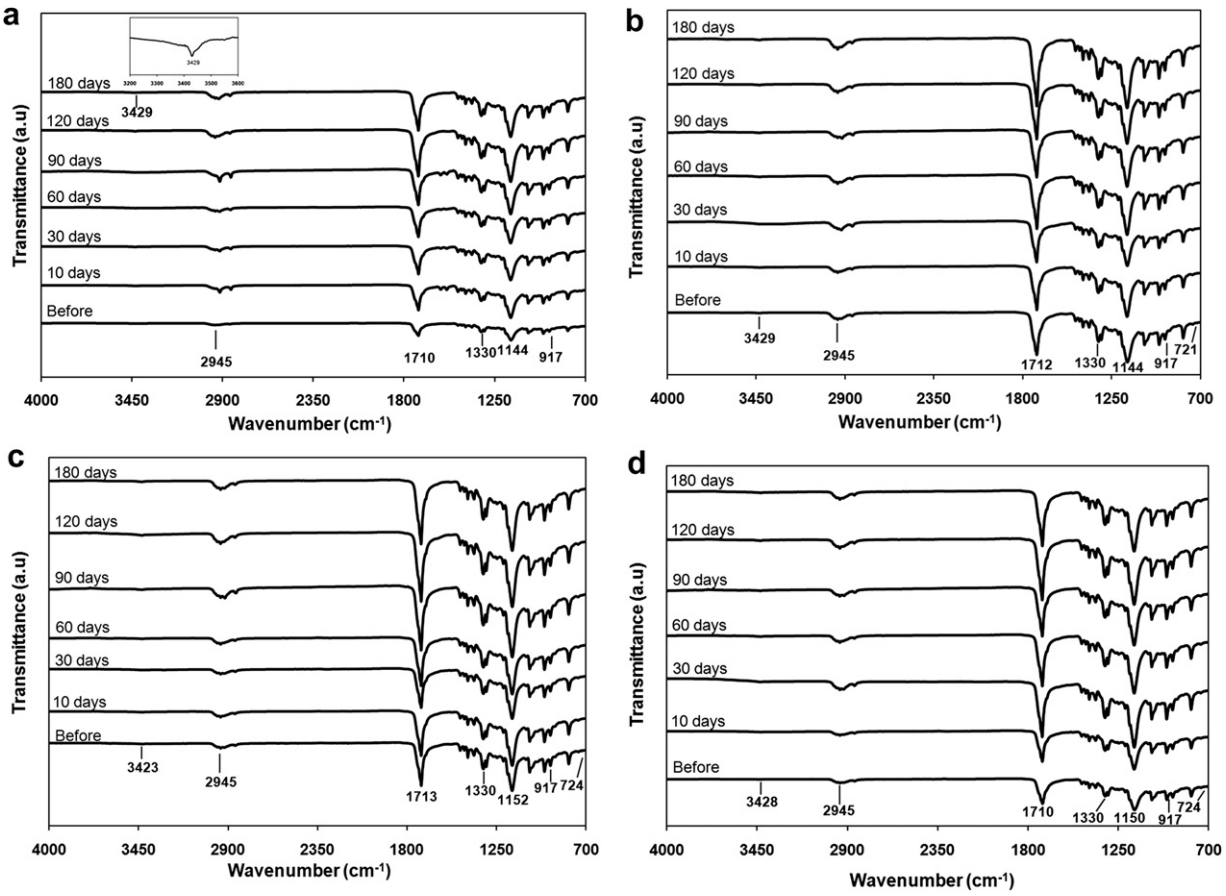

Fig. 7. FTIR spectra of (a) neat PBS, (b) PBS/2%OMMT, (c) PBS/10%OMMT and (d) compatibilised nanocomposites at various soil burial time.

of chain scission in the PBS chains, which is associated with the formation of more carboxylic end groups and ketone species [31,32]. In the same way, the formation of vinyl groups is the result of polymer chain scission, as verified by the higher VI after biodegradation. The segments formed during the chains ruptured by the attack of microorganism led to the formation of the vinyl groups [33]. Besides that, the increased HI with soil burial time is likely caused by the generation of hydroperoxide species and alcohol end groups after soil burial [32]. Before soil burial, nanocomposites demonstrated higher HI as compared to neat PBS, due to the presence of OH groups on the OMMT surface. The CI, VI and HI showed a decrement after 60–90 days of soil burial, which is believed to be due to materials leaching from the sample surface. The process of biodegradation may also convert the polymer to other elements such as CO_2 and water after being metabolized by microorganism, and reduced the CI, VI and HI values. Based on the above observations and analysis, it is proposed that the mechanism of PBS biodegradation is as shown in Fig. 8.

Table 3
Carbonyl, vinyl and hydroxyl indexes of PBS and the nanocomposites at various soil burial time.

Compound	Buried time (day)						
	0	10	30	60	90	120	180
Carbonyl index (CI)							
PBS	6.53	7.23	7.76	7.66	7.87	6.41	6.09
PBS/2%OMMT	6.10	6.24	6.42	6.65	6.72	6.59	6.47
PBS/10%OMMT	6.16	7.74	7.73	7.82	7.30	6.41	6.65
PBS/2%OMMT/MA	6.54	7.22	7.23	7.26	8.23	6.98	6.77
Vinyl index (VI)							
PBS	3.85	4.20	4.26	4.76	4.12	3.14	3.18
PBS/2%OMMT	3.37	3.57	3.50	3.71	3.43	3.07	3.02
PBS/10%OMMT	3.77	4.20	4.31	4.36	3.39	3.18	3.26
PBS/2%OMMT/MA	3.83	4.27	4.30	4.41	3.89	3.32	3.41
Hydroxyl index (HI)							
PBS	0.13	0.13	0.14	0.21	0.20	0.14	0.11
PBS/2%OMMT	0.17	0.22	0.21	0.25	0.28	0.10	0.10
PBS/10%OMMT	0.19	0.24	0.23	0.28	0.37	0.22	0.19
PBS/2%OMMT/MA	0.18	0.19	0.29	0.29	0.41	0.2	0.17

3.6. Gel permeation chromatography (GPC)

The molecular weight degradation is a permanent damage caused by irreversible chemical reactions that occur during the biodegradation of polymers [34]. Therefore, the measurement of molecular weight was conducted using GPC technique in order to determine the extent of biodegradation quantitatively. During the 180 days of soil burial, a continuous reduction in weight-average molecular weight (M_w) and number-average molecular weight (M_n) was observed (Table 4). Generally, biodegradation process occurs in two key steps: depolymerization or chain cleavage step, and mineralization. The enzymes produced by microorganisms first hydrolyse the ester linkages in the PBS chains via chain scission, resulting in smaller sized oligomeric, dimeric or monomeric fragments. This is followed by the mineralisation of polymer by microbial metabolism, leading to the complete breakdown of the polymer to carbon dioxide, water and biomass [35,36]. Therefore, the decrease in molecular weight confirms the occurrence of chain scission in PBS due to hydrolysis and microbial attack. The extent of

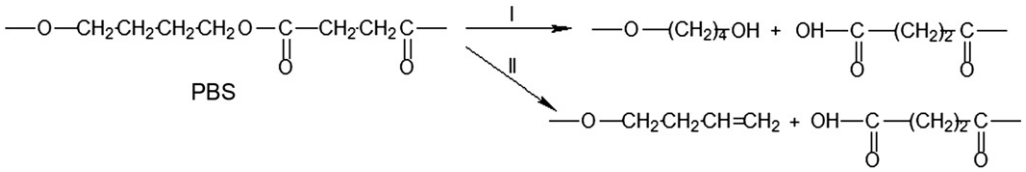

Fig. 8. Proposed mechanism of biodegradation on PBS.

Table 4
GPC results of PBS at various soil burial time.

Buried time	M_w (g/mol)	M_n (g/mol)	PDI	n_t (mol/g)
Before	21,168	42,128	1.99	–
90 days	18,705	39,015	2.09	6.22×10^{-6}
180 days	8924	23,380	2.62	6.48×10^{-5}

chain scission was further quantified through the average number of random chain scissions per unit mass (n_t). The result shows that chain scission occurred continuously during the soil burial, leading to a higher number of chain scission as the buried time increased.

Polydispersity index (PDI) is a measure of the molecular weight distribution in a polymer. From Table 4, it is noted that PDI increased significantly with the exposure time to soil burial. The random chain scission in the PBS backbone caused a greater variation in the polymer chain length, subsequently resulting in the broadening of molecular weight distribution [37,38].

3.7. Carbon dioxide (CO_2) evolution

Mineralisation occurs when the polymer chains are metabolised by microorganisms after the initial chain scission process to carbon dioxide (CO_2), water, and biomass [35,36]. Hence, the degree of aerobic biodegradation can be determined by measuring the CO_2 evolved as a function of time that the polymers were exposed to soil [39,40]. It is observed that the positive control (starch) reached 100% of mineralisation in 180 days, validating the test according to ASTM D5988. The cumulative CO_2 evolution curves for PBS and the nanocomposites are shown in Fig. 9, where the biodegradation rate is referred as the slope of the tangent to each curve. It can be seen that the CO_2 evolution increased at a relatively rapid rate during the first 83 days, followed by a gradual decreasing rate with time during the remaining period of the exposure. The rapid biodegradation rate at the initial stage is ascribed to the degradation of low molecular weight fragments, amorphous region, as well as the exposed end groups in PBS [18]. In agreement with the previous discussion, neat PBS attained the highest biodegradation rate with a total of 65.2% CO_2 evolution after 180 days of soil burial. The compatibilised nanocomposites, PBS/10%OMMT and PBS/2%OMMT nanocomposites exhibit a total of 62.7%, 57.8% and 50.2% CO_2 evolution, respectively. This is in line with the previous observations that the incorporation of OMMT reduced the biodegradability, while the addition of PBS-g-MA promotes the biodegradation of the material.

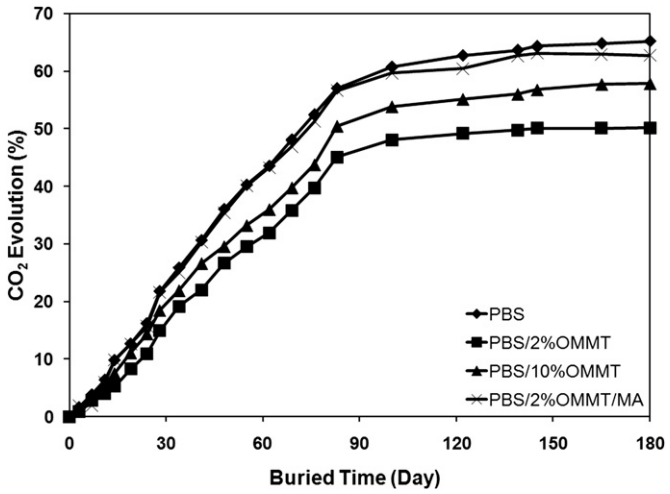

Fig. 9. Cumulative carbon dioxide evolution of PBS and the nanocomposites as a function of buried time.

ASTM 5988 does not address clear specifications on the overall level of biodegradation that must be achieved to claim a material is biodegradable. However, according to ASTM D6400, a material may be considered degradable only when it reaches 60% of CO_2 evolution in a period of 180 days [41]. From the results, only neat PBS and compatibilised nanocomposites reached this point by the end of the test period. This reflects the facts that PBS-g-MA functions as a potential compatibiliser for PBS nanocomposites due to its ability to improve the mechanical properties without compromising the biodegradability of PBS. It is also believed that the selection of soil and the exposed conditions play an important role in the biodegradation process.

3.8. Isolation and identification of bacterial strain

After 180 days of soil burial, the PBS samples were analysed to determine the microbial populations that were present on the samples. A homology search was performed to compare the obtained 16S rDNA sequences with the GenBank database. The predominant bacteria identified from the buried PBS samples were *Bacillus* sp., *Ammoniphilus* sp., and *Cupriavidus* sp. These bacteria have long been known as soil bacteria [42,43]. *Bacillus* sp. is a gram positive, rod-shaped bacterium that was often reported as one of the PBS degraders by numerous researchers [44,45]. This bacterium utilizes PBS as sole source of carbon and results in the degradation of PBS. In a previous polymer ageing study, *Aminophilus* sp. CC-RT-E was isolated from aged resin of tropical rainforest (Accession no. HM193518). Various bacteria have been reported to degrade PBS efficiently e.g. *Bacillus stearothermophilus*, *Microbispora rosea*, *Excellospora japonica*, *Excellospora viridilutea*, *Penicillium chrysogenum*, *Bacillus pumilus*, *Acidovorax delafieldii*, *Aspergillus versicolor* and etc. [44–46]. Hence, it is speculated that the *Bacillus* sp. that were identified from the soil-buried PBS samples may be involved in the degradation of the samples. However, there are no reports on the ability of *Cupriavidus* sp. and *Ammoniphilus* sp. to degrade PBS. Therefore, further studies are required to determine the ability of these bacteria in degrading PBS.

4. Conclusions

Biodegradation of PBS and the nanocomposites occurred over a period of 180 days of soil burial testing. The action of moisture and microorganism in soil caused the partial disruption of filler-matrix bonding, microcavities formation and was followed by a random

chain scission in the polymer chains. These changes were accompanied by significant loss in weight, mechanical properties and molecular weight of the samples. PBS nanocomposites showed lower biodegradability than that of neat PBS due to improved barrier properties. However, the extent of biodegradation is greatly dependent on the OMMT dispersion in PBS matrix, where agglomerations at high OMMT loading diminished the barrier effects. The addition of PBS-g-MA as compatibiliser enhanced the biodegradability of the nanocomposites, because of its chemical structure and low molecular weight. The biodegradability of PBS and its nanocomposites were further confirmed through SEM observations and CO_2 evolution measurements. The results suggested that that PBS-g-MA worked as a potential compatibiliser for PBS nanocomposites by enhancing both the mechanical properties and the biodegradability of PBS. On the other hand, the DSC results showed that thermal behaviours of PBS and the nanocomposites were affected after soil burial. The T_c and χ_c decreased after soil burial, indicating that biodegradation takes place in both the amorphous and the crystalline regions in PBS. The FTIR analysis demonstrated the structural changes in PBS and the nanocomposites. Higher quantity of carbonyl groups, vinyl groups and hydroxyl groups were produced after biodegradation. These results confirmed the biodegradability of PBS and the nanocomposites in compost soil, which support the role of PBS as a potential biodegradable material in various applications. Among the various microorganisms found on the buried samples, *Bacillus*, which is a known class of PBS-degrading bacteria, was also identified by colony PCR technique.

Acknowledgements

The financial support of USM Research University Cluster Grant (1001/PKT/8640012), USM Incentive Grant (1001/PBAHAN/8021011), USM Research University Postgraduate Research Grant Scheme (1001/PBAHAN/8044004) and USM Fellowship is gratefully acknowledged.

References

[1] Okamoto K, Ray SS, Okamoto M. New poly(butylene succinate)/layered silicate nanocomposites. II. Effect of organically modified layered silicates on structure, properties, melt rheology, and biodegradability. Journal of Polymer Science, Part B: Polymer Physics 2003;41(24):3160–72.
[2] Someya Y, Nakazato T, Teramoto N, Shibata M. Thermal and mechanical properties of poly(butylene succinate) nanocomposites with various organo-modifies montmorillonites. Journal of Applied Polymer Science 2003;91(3):1463–75.
[3] Chen GX, Kim ES, Yoon JS. Poly(butylene succinate)/twice functionalized organoclay nanocomposites: preparation, characterization, and properties. Journal of Applied Polymer Science 2005;98(4):1727–32.
[4] Fujimaki T. Processability and properties of aliphatic polyesters, 'BIONOLLE', synthesized by polycondensation reaction. Polymer Degradation and Stability 1998;59(1–3):209–14.
[5] Chieng BW, Ibrahim NA, Wan Yunus WMZ. Effect of organo-modified montmorillonite on poly(butylene succinate)/poly(butylene adipate-co-terephthalate) nanocomposites. Express Polymer Letters 2010;4(7):404–14.
[6] Phua YJ, Chow WS, Mohd Ishak ZA. Poly(butylene succinate)/organo-montmorillonite nanocomposites: effects of the organoclay content on mechanical, thermal, and moisture absorption properties. Journal of Thermoplastic Composite Materials 2010;24(4):133–51.
[7] Phua YJ, Chow WS, Mohd Ishak ZA. Mechanical properties and structure development in poly(butylene succinate)/organo-montmorillonite nanocomposites under uniaxial cold rolling. Express Polymer Letters 2011;5(2):93–103.
[8] Nishide H, Toyota K, Kimura M. Effects of soil temperature and anaerobiosis on degradation of biodegradable plastics in soil and their degrading microorganisms. Soil Science and Plant Nutrition 1999;45:963–72.
[9] Kitakuni E, Yoshikawa K, Nakano K, Sasuga J, Nobiki M, Naoi H, et al. Biodegradation of poly(tetramethylene succinate-co-tetramethylene adipate) and poly(tetramethylene succinate) through water-soluble products. Environmental Toxicology and Chemistry 2001;20:941–6.
[10] Tezuka Y, Ishii N, Kasuya K, Mitomo H. Degradation of poly(ethylene succinate) by mesophilic bacteria. Polymer Degradation and Stability 2004;84:115–21.
[11] Kim HS, Yang HS, Kim HJ. Biodegradability and mechanical properties of agro-flour filled polybutylene succinate biocomposites. Journal of Applied Polymer Science 2005;97:1513–21.
[12] Yabannavar AV, Bartha R. Methods for assessment of biodegradability of plastic films in soil. Applied and Environmental Microbiology 1994;60:3608–14.
[13] Domenek S, Feuilloley P, Gratraud J, Morel MH, Guilbert S. Biodegradability of wheat gluten based bioplastics. Chemosphere 2004;54:551–9.
[14] Kijchavengkul T, Auras R, Rubino M, Selke S, Ngouajio M, Fernandez RT. Biodegradation and hydrolysis rate of aliphatic aromatic polyester. Polymer Degradation and Stability 2010;95:2641–7.
[15] Liu L, Yu J, Cheng L, Yang X. Biodegradablity of poly(butylene succinate) (PBS) composite reinforced with jute fibre. Polymer Degradation and Stability 2009;94:90–4.
[16] Phua YJ, Chow WS, Mohd Ishak ZA. The hydrolytic effect of moisture and hygrothermal aging on poly(butylene succinate)/organo-montmorillonite nanocomposites. Polymer Degradation and Stability 2011;96(7):1194–203.
[17] Annick W, Auwera GVD, Wachter RD. Structure of the 16 S ribosomal RNA of the thermophilic cyanobacterium Chlorogloeopsis HTF ('Mastigocladus laminosus HTF') strain PCC7518, and phylogenetic analysis. Federation of European Biochemical Societies, Volume 317, number 1,2, 96–100.
[18] Thellen C, Orroth C, Froio d, Ziegler D, Lucciarini J, Farrell R, et al. Influence of montmorillonite layered silicate on plasticized poly(L-lactide) blown films. Polymer 2005;46:11716–27.
[19] Lee SR, Park HM, Lim H, Kang T, Li X, Cho WJ, et al. Microstructure, tensile properties, and biodegradability of aliphatic polyester/clay nanocomposites. Polymer 2002;43:2495–500.
[20] Frounchi M, Dadbin S, Salehpour Z, Noferesti M. Gas barrier properties of PP/EPDM blend nanocomposites. Journal of Membrane Science 2006;282:142–8.
[21] Jang WY, Shin BY, Lee TJ, Narayan R. Thermal properties and morphology of biodegradable PLA/Starch compatibilised blends. Journal of Industrial and Engineering Chemistry 2007;13:457–64.
[22] Vlasveld DPN, Groenewold J, Bersee HEN, Picken SJ. Moisture absorption in polyamide-6 silicate nanocomposites and its influence on the mechanical properties. Polymer 2005;46(26):12567–76.
[23] Qiu Z, Ikehara T, Nishi T. Poly(hydroxybutyrate)/poly(butylene succinate) blends: miscibility and nonisothermal crystallization. Polymer 2003;44(8):2503–8.
[24] Ray SS, Bousmina M, Okamoto K. Structure and properties of nanocomposites based on poly(butylene succinate-co-adipate) and organically modified montmorillonite. Macromolecular Materials and Engineering 2005;290(8):759–68.
[25] Pang MZ, Qiao JJ, Jiao J, Wang SJ, Xiao M, Meng YZ. Miscibility and properties of completely biodegradable blends of poly(propylene carbonate) and poly(-butylene succinate). Journal of Applied Polymer Science 2008;107(5):2854–60.
[26] Lee SM, Jeon HJ, Choi SW, Song HH. Structure and property modification of bimodal molecular weight distribution polyethylene by electron beam irradiation. Macromolecular Research 2006;14:640–5.
[27] Kim HS, Kim HJ, Lee JW, Choi IG. Biodegradability of bio-flour filled biodegradable poly(butylene succinate) bio-composites in natural and compost soil. Polymer Degradation and Stability 2006;91:1117–27.
[28] Rabello MS, White JR. Crystallization and melting behaviour of photodegraded polypropylene. 2. Recrystallization of degraded molecules. Polymer 1997;38:6389–99.
[29] Wang M, Zhao F, Guo Z, Dong S. Poly(vinylidene fluoride-hexafluoropropylene)/organo-montmorillonite clays nanocomposite lithium polymer electrolytes. Electrochim Acta 2004;49(21):3595–602.
[30] Tidjani A. Comparison of formation of oxidation products during photo-oxidation of linear low density polyethylene under different natural and accelerated weathering conditions. Polymer Degradation and Stability 2000;68:465–9.
[31] Kumar R, Yakubu MK, Anandjiwala RD. Biodegradation of flax fiber reinforced poly lactic acid. Express Polymer Letters 2010;4:423–30.
[32] Ahmad Thirmizir MZ, Mohd Ishak ZA, Mat Taib R, Rahim S, Mohamad Jani S. Natural weathering of kenaf bast fibre-filled poly(butylene succinate) composites: effect of fibre loading and compatibiliser addition. Journal of Polymers and the Environment 2011;19:263–73.
[33] Manzur A, Limón-González M, Favela-Torres E. Biodegradation of physico-chemically treated LDPE by a consortium of filamentous fungi. Journal of Applied Polymer Science 2004;92:265–71.
[34] Mohd Ishak ZA, Berry JP. Hygrothermal aging studies of short carbon fiber reinforced nylon 6.6. Journal of Applied Polymer Science 1994;51(13):2145–55.
[35] Moore GF, Saunders SM. Advances in biodegradable polymers. p. 7–12. United Kingdom: Rapra Technology Ltd; 1998.
[36] Premraj R, Doble M. Biodegradation of polymers. Indian Journal of Biotechnology 2005;4:186–93.
[37] He Z, Xiong L. A comparative study on in vitro degradation behaviours of poly(L-lactide-co-glycolide) scaffolds and films. Journal of Macromolecular Science, Part B: Physics 2010;49:66–74.

[38] Ndazi BS, Karlsson S. Characterization of hydrolytic degradation of polylactic acid/rice hulls composites in water at different temperatures. Express Polymer Letters 2011;5:119–31.
[39] Modelli A, Calcagno B, Scandola M. Kinetics of aerobic polymer degradation in soil by means of the ASTM D 5988-96 standard method. Journal of Environmental Polymer Degradation 1999;7:109–16.
[40] Calmon A, Dusserre-Bresson L, Bellon-Maurel V, Feuilloley P, Silvestre F. An automated test for measuring polymer biodegradation. Chemosphere 2000; 41:645–51.
[41] Mariani PDSC, Neto Jr APV, Cardoso EJBN, Esposito E, Innocentini-Mei LH. Mineralization of poly(ε-caprolactone)/adipate modified starch blend in agricultural soil. Journal of Polymers and the Environment 2007;15: 19–24.
[42] Hong HA, To E, Fakhry S, Baccigalupi L, Ricca E, Cutting SM. Defining the natural habitat of Bacillus spore-formers. Research in Microbiology 2009;160:375–9.
[43] Ishii S, Yamamoto M, Tago K, Otsuka S, Senoo K. Microbial populations in various paddy soils respond differently to denitrification-inducing conditions, albeit background bacterial populations are similar. 2010. 56, 220–224.
[44] Tomita K, Kuroki Y, Hayashi N, Komukai Y. Isolation of a thermophile degrading poly(butylene succinate-co-butylene adipate). Journal of Bioscience and Bioengineering 2000;90:350–2.
[45] Hayase N, Yano H, Kudoh E, Tsutsumi C, Ushio K, Miyahara Y, et al. Isolation and characterization of poly(butylene succinate-cobutylene adipate)-degrading microorganism. Journal of Bioscience and Bioengineering 2004;97:131–3.
[46] Tokiwa Y, Calabia BP, Ugwu CU, Aiba S. Biodegradability of plastics. International Journal of Molecular Sciences 2009;10:3722–42.